

ison with more standard GAs. The suitability of the identified model was demonstrated by showing its predictive capabilities against tests with significantly different mass distributions.

### References

- <sup>1</sup>Kabe, A. M., "Stiffness Matrix Adjustment Using Mode Data," *AIAA Journal*, Vol. 23, No. 9, 1985, pp. 1431–1436.
- <sup>2</sup>Doyle, J. F., "A Genetic Algorithm for Determining the Location of Structural Impacts," *Experimental Mechanics*, March 1994, pp. 37–44.
- <sup>3</sup>Larson, C. B., and Zimmerman, D. C., "Structural Model Refinement Using a Genetic Algorithm Approach," *Proceedings of the 11th International Modal Analysis Conference* (Kissimmee, FL), Society for Experimental Mechanics, Bethel, CT, 1993, pp. 1095–1101.
- <sup>4</sup>Dunn, S. A., "The Use of Genetic Algorithms and Stochastic Hill-Climbing in Dynamic Finite-Element Model Identification," *Computers and Structures* (submitted for publication).
- <sup>5</sup>KrishnaKumar, K., "Micro Genetic Algorithms for Stationary and Non-Stationary Function Optimization," *SPIE Proceedings Volume 1196*, SPIE Intelligent Control and Adaptive Systems Meeting (Philadelphia, PA), Society of Photo-Optical Instrumentation Engineers, Paper 1196-32, 1989.

## Induced Drag Computations on Wings with Accurately Modeled Wakes

Stephen C. Smith\*  
NASA Ames Research Center,  
Moffett Field, California 94035

and

Ilan M. Kroo†  
Stanford University, Stanford, California 94305

### Introduction

THE trailing wake model employed by classical finite wing theory is a thin vorticity sheet that leaves the trailing edge in the freestream direction. Although this straight wake differs from the physical, force-free wake shape, it is drag free, since the wake vorticity is parallel to the freestream. This fact enables accurate induced drag computation with straight wakes by integration of the wake properties in the Trefftz plane. The use of straight wakes in linear potential methods is well established, providing sufficient accuracy for most engineering analyses.

Although the potential for reducing drag may be small, the influence of the force-free wake on induced drag has become the subject of active research. A study of the nonlinear effects of wake shape on induced drag requires Trefftz-plane integration on the force-free wake. However, any error in the computed wake shape will produce an error in the integrated drag, since the wake is no longer force-free. This Note presents a novel wake relaxation scheme that was developed to enable accurate Trefftz-plane integration of induced drag with force-free wakes.

Received June 17, 1996; revision received Nov. 8, 1996; accepted for publication Nov. 18, 1996. Copyright © 1996 by the American Institute of Aeronautics and Astronautics, Inc. No copyright is asserted in the United States under Title 17, U.S. Code. The U.S. Government has a royalty-free license to exercise all rights under the copyright claimed herein for Governmental purposes. All other rights are reserved by the copyright owner.

\*Research Engineer, High Speed Aerodynamics Branch. Member AIAA.

†Associate Professor. Member AIAA.

### Background

References 1–3 have demonstrated that surface-pressure integration is an unreliable method of computing induced drag. Errors arising from inadequate resolution of the pressure distribution may be planform dependent, leading to incorrect conclusions about the influence of planform shape on induced drag.<sup>1,2</sup> When panel methods are used, the induced drag may be determined by surveying the trailing wake properties and numerically evaluating the well-known Trefftz plane integral. Reference 1 described the application and accuracy of this technique using the Boeing A502 high-order panel code.<sup>4</sup> All induced drag values presented in this Note were computed by this technique.

Linear panel methods require that the wake geometry be prescribed, and so either a straight wake model or a model of the force-free wake shape must be obtained. A variety of techniques exist for computing the force-free wake shape downstream of the wing. The most widely used methods use a discrete vortex-lattice model of the wing and wake.<sup>5–7</sup> The velocities induced on the wake are computed and an iterative procedure is used to displace the wake to align it with the local flow. A viscous core model is required to prevent erratic behavior of the vortex filaments when they pass near each other. Reference 8 describes an alternative method of relaxing a distributed-vorticity wake sheet, using a smoothing algorithm to prevent erratic behavior along the outboard edge. Once the force-free wake shape is created, it can then be converted to a panel geometry for Trefftz plane drag analysis by the high-order panel code.

### Errors Associated with Vortex-Lattice Wake Relaxation Schemes

A time-marching vortex-lattice wake relaxation program<sup>5</sup> was used to create a force-free wake model for an elliptical wing [aspect ratio, (AR) = 7, with straight trailing edge] at 4.0-deg angle of attack. This wing was chosen based on a hypothesis described in Refs. 9 and 10, indicating that a straight wake model and an accurate force-free wake model should produce the same Trefftz-plane drag for this planform. A panel model of the same wing was created with NACA 0012 airfoils and a panel representation of the force-free wake geometry from the vortex-lattice method. The 50-vortex model of the wake was edited to match the 18 spanwise panels on the wing. Convergence studies in Ref. 1 indicate that the expected error in numerical evaluation of the Trefftz-plane integral with 18 panels is about 0.5%. Since the wing lift (circulation) rather than angle of attack determines the wake shape, the angle of attack of the panel model was adjusted to match the lift coefficient of the vortex-lattice model.

The computed span efficiency,  $e = C_L^2 / \pi AR C_{D_i}$ , of this model was 1.035, almost 5% higher than the expected value based on the straight wake result,  $e = 0.99$ . To improve the resolution of the wake shape, the 50-vortex wake model was re-edited to create a model with 19 spanwise panels. This produced a computed  $e = 1.058$ . A second vortex-lattice wake model was then generated with half the time-step size, again to improve the resolution of the wake shape. A 19-panel representation of this wake produced a computed  $e = 1.082$ , 9% higher than the expected value. The small change in wake shape that produced this large change in computed span efficiency is shown in Fig. 1. Evidently, the drag computed in the Trefftz plane is highly sensitive to details of the wake shape.

One possible source of error in wake shape is the approximation of the wing flowfield inherent to the vortex-lattice method. The wake shape is determined from velocities induced by the bound and trailing vortex systems, but vortex-lattice methods have velocity singularities at the panel edges, and the velocities are correct only at the control points. Significant velocity errors exist at other points in the field, particularly at

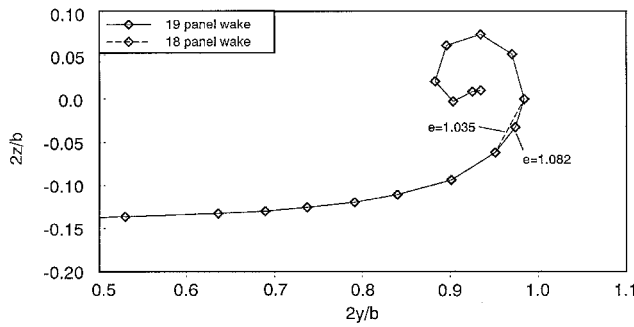


Fig. 1 Computed span efficiency affected by small change in wake shape.

the trailing edge. If velocity errors exist on the wake near the trailing edge, the relaxed wake shape would be incorrect.

Further difficulty with the discrete-vortex representation of the wing arises when the wake passes near a portion of wing surface, such as the case of a closely coupled tandem wing. In this case, the velocity singularities on the wing produce highly erratic behavior of the wake vortex filaments as they pass over the wing. To study the potential for nonlinear interaction of the wake and wing surface, a more reliable method for computing the force-free wake shape is needed.

### Hybrid Wake-Relaxation Scheme

One method of improving the velocities near the trailing edge is a hybrid wake-relaxation method that takes advantage of the more accurate velocities of the high-order panel method while exploiting the well-behaved nature of the discrete-vortex wake with viscous-core model. The high-order panel method is used to compute the velocities induced on the wake by the wing, whereas the velocities induced by the wake itself are computed from the discrete-vortex model. The wake vortex strengths are determined from the vorticity distribution on the wake from the panel code. A relaxation scheme iteratively repositions the wake to be tangent to the local flow.

A flow chart of the iteration process used to relax the wake shape is shown in Fig. 2. At the beginning of each iteration, a complete flow solution for the wing and wake geometry is obtained from the high-order panel code. The aerodynamic influence coefficient matrix (AIC) and the singularity strengths  $\{\mu\}$  for this solution are saved to permit evaluation of field velocities. The wake circulation distribution is determined and an equivalent discrete-vortex wake is constructed. A downstream space-march is then used to convect the wake to align it with the local flow. Velocities induced by the wing system (not including the wake) along a spanwise row of nodes on the wake are computed from the saved AICs and singularity strengths from the panel code. The velocities induced by the discrete-vortex wake are computed at the same nodes using the Biot-Savart law, modified by the viscous-core model of Ref. 5. The induced velocities from the wing system and wake are then combined to form the total induced velocities,  $v$  and  $w$ , needed to convect the wake.

A second-order Adams-Bashforth method is used to determine the displacement of the next row of nodes so that the intervening wake segments are tangent to the local flow. Although the convergence rate is reduced, the method is more robust if the nodal displacement is reduced by an underrelaxation factor  $r$ . At each step in the space-march, the entire wake downstream of the current set of nodes is displaced, allowing the evolving wake shape to propagate downstream. This method, applied to the  $z$  component of the wake position, can be summarized mathematically as follows:

$$Z_{i+1}^* = Z_i^n + \frac{dx}{U_\infty} \left( \frac{3}{2} w_i - \frac{1}{2} w_{i-1} \right)$$

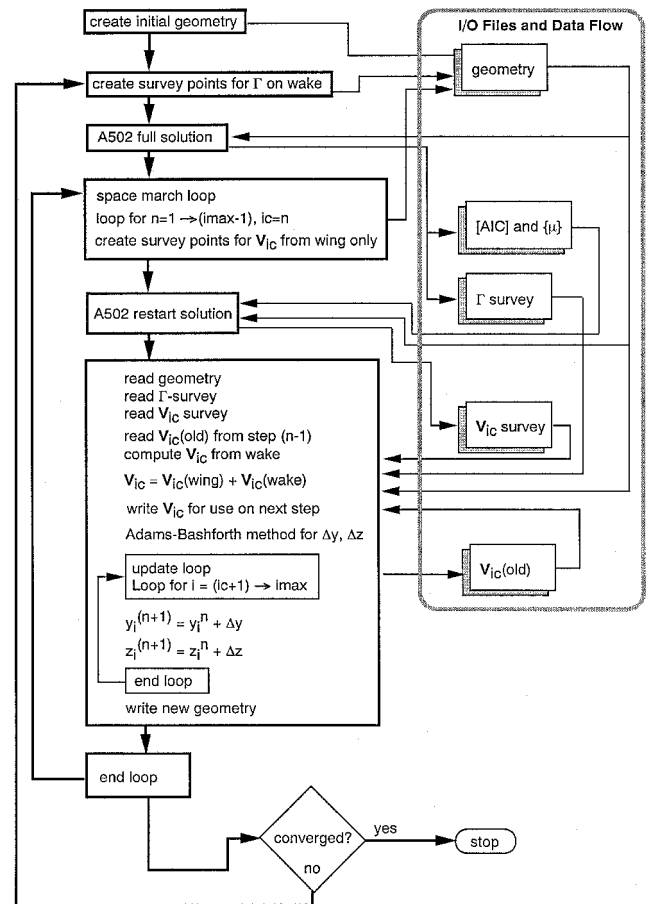


Fig. 2 Flow chart of hybrid wake relaxation scheme.

where  $i$  is the current node index

$$dz = r(Z_{i+1}^* - Z_{i+1}^n)$$

where  $n$  is the marching index and  $r$  is the relaxation factor, and finally, the nodal displacements are applied at all nodes downstream:

$$Z_{i+1 \rightarrow imax}^{n+1} = Z_{i+1 \rightarrow imax}^n + dz$$

The same procedure is applied to the  $y$  component.

Once this marching process propagates to the downstream boundary of the wake, the next iteration begins with a new flow solution from the panel code with the revised wake geometry. The update of the AICs and singularity strengths is necessary because the wake displacement modifies the influence of the wake on the wing. Experience with this method has shown that convergence to a qualitatively reasonable wake shape takes three or four iterations, but convergence of the Trefftz-plane drag computation to within 0.25% requires 12–15 iterations, using an underrelaxation value of  $r = 0.5$ .

### Sample Results

This hybrid wake-relaxation scheme was applied to two AR = 7 elliptical wing planforms, with complete results presented in Ref. 1. Trefftz-plane induced-drag predictions were obtained with a straight wake model as well as with force-free wakes generated by the hybrid scheme and the previously described vortex-lattice method. For the wing with straight trailing edge, a comparison of the wake shapes and span efficiency determined by the two wake relaxation methods is shown in Fig. 3. Drag predictions from high-resolution pressure integrations for the straight wake model and the force-free wake model

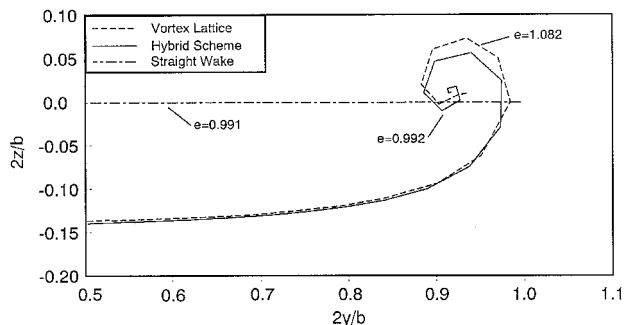


Fig. 3 Wake shapes produced by vortex-lattice and hybrid methods.

agreed within 0.1%, consistent with the hypothesis of Refs. 9 and 10. The agreement of the Trefftz-plane drag computed with the straight wake and the force-free wake, also 0.1%, indicates that the hybrid scheme produces force-free wakes of sufficient accuracy to enable Trefftz-plane integration of drag.

The hybrid method has also been successfully applied to an unusual split tip wing that has two outer wing panels in tandem, with no dihedral.<sup>10</sup> This planform is challenging for the wake-relaxation method because the wake from the forward tip panel passes closely over the rear tip panel. A conventional vortex-lattice method could not accommodate this close wake interaction because of the strong velocity singularities produced by the vortex elements on the wing. The drag prediction for the split tip wing using the hybrid wake method was in close agreement with high-resolution pressure integration as well as with wind-tunnel experiments using a wake survey method that enables direct measurement of induced drag.

### Conclusions

A technique has been developed for numerically computing the force-free wake shape downstream of finite wings, based on the need for very accurate integration of induced drag in the Trefftz plane. An AR = 7 elliptical wing with straight trailing edge was used to study the influence of the computed wake shape on induced drag. A traditional vortex-lattice relaxation method produced a wake that led to a 9% error in Trefftz-plane drag. The new method presented here obtains more accurate wing-induced velocities from a high-order panel method, while relying on the well-behaved nature of the discrete-vortex wake model for the wake-induced velocities. The induced drag with the wake produced by this hybrid scheme agreed with the drag predicted with a straight wake within 0.1%, consistent with high-resolution pressure integration. These and other cited results indicate that the hybrid scheme produces wakes of sufficient accuracy to enable Trefftz-plane integration of drag on the force-free wake.

### References

- <sup>1</sup>Smith, S. C., and Kroo, I. M., "Computation of Induced Drag for Elliptical and Crescent-Shaped Wings," *Journal of Aircraft*, Vol. 30, No. 4, 1993, pp. 446–452.
- <sup>2</sup>Dehaan, M. A., "Induced Drag of Wings with Highly Swept and Tapered Wing Tips," AIAA Paper 90-3062, Aug. 1990.
- <sup>3</sup>Letcher, J. S., Jr., "Convergence of Lift and Drag Predictions by a Morino Panel Method (VSAERO)," *AIAA Journal*, Vol. 27, No. 8, 1989, pp. 1019, 1020.
- <sup>4</sup>Carmichael, R. L., and Erickson, L. L., "PANAI—A Higher Order Panel Code for Predicting Subsonic or Supersonic Linear Potential Flows About Arbitrary Configurations," AIAA Paper 81-1255, June 1981.
- <sup>5</sup>Mittelman, Z., "Prediction of Unsteady Aerodynamics and Control of Delta Wings with Tangential Leading Edge Blowing," Ph.D. Dissertation, Stanford Univ., SUDDAR-580, Stanford, CA, June 1989.
- <sup>6</sup>Quackenbush, T. R., Bliss, D. B., Wachspress, D. A., and Ong, C. C., "Free Wake Analysis of Hover Performance Using a New Influence Coefficient Method," NASA CR 4309, July 1990.

<sup>7</sup>Ashby, D. L., Dudley, M. R., and Iguchi, S. K., "Development and Validation of an Advanced Low-Order Panel Method," NASA TM 101024, Oct. 1988.

<sup>8</sup>Nagati, M. G., Iverson, J. D., and Vogel, J. M., "Vortex Sheet Modeling with Curved Higher-Order Panels," *Journal of Aircraft*, Vol. 24, No. 11, 1987, pp. 776–781.

<sup>9</sup>Kroo, I. M., and Smith, S. C., "Computation of Induced Drag with Nonplanar and Deformed Wakes," Society of Automotive Engineers Transactions, Paper 901933, Sept. 1990.

<sup>10</sup>Smith, S. C., "A Computational and Experimental Study of Non-linear Aspects of Induced Drag," NASA TP 3598, Feb. 1996.

## New Blunt Trailing-Edge Airfoil Design by Inverse Optimization Method

Shigeru Obayashi\* and Shinkyu Jeong†  
Tohoku University, Sendai 980-77, Japan  
and

Yuichi Matsuo‡  
National Aerospace Laboratory, Chofu 182, Japan

### Introduction

**A**ERODYNAMIC shape optimization is one of the major targets of computational fluid dynamics (CFD) today to improve design efficiency. Among aircraft components, optimization of airfoil shape has a significant impact on aircraft performance. Thus, transonic airfoil optimization is considered here.

In Ref. 1, a genetic algorithm (GA) has been applied to optimize target pressure distributions for inverse design methods. Pressure distributions around airfoils are parameterized by B-spline polygons, and the airfoil drag is minimized under constraints on lift, airfoil thickness, and other design principles. Once a target pressure distribution is obtained, corresponding airfoil geometry can be computed by an inverse design code coupled with a Navier–Stokes solver. Successful design results were obtained for transonic cases with and without a shock wave. In Ref. 1, a sharp trailing edge was employed for airfoil closure.

Traditionally, airfoil closure has been accomplished by using a sharp trailing edge. Work to develop the supercritical airfoil has shown the possibility of using a thin trailing-edge geometry with near-parallel trailing-edge surfaces to produce a superior transonic airfoil section. Further study by Henne<sup>2</sup> leads to a divergent trailing-edge airfoil that utilizes the bluntness of the trailing edge to improve transonic performance. Flowfields around such blunt trailing-edge airfoils have been studied numerically in Refs. 3–5.

In Ref. 6, the inverse optimization method was extended to the design of blunt trailing-edge airfoils. To predict the flowfield around the blunt trailing edge accurately, a grid was placed in the wake region behind the blunt trailing edge (the *H* grid) in addition to a grid wrapping around the airfoil sur-

Received Aug. 28, 1996; revision received Nov. 12, 1996; accepted for publication Nov. 18, 1996. Copyright © 1996 by the American Institute of Aeronautics and Astronautics, Inc. All rights reserved.

\*Associate Professor, Department of Aeronautics and Space Engineering. E-mail: obayashi@ad.mech.tohoku.ac.jp. Senior Member AIAA.

†Graduate Student, Department of Aeronautics and Space Engineering.

‡Senior Scientist, Computational Sciences Division. Member AIAA.